18. THE LINK TO AN EXTRAGALACTIC SYSTEM

The positions and proper motions in the Hipparcos and Tycho Catalogues refer to the International Celestial Reference System, ICRS. This means that the coordinate axes of the catalogues have been aligned with the reference frame determined through VLBI radio observations of extragalactic sources, and remain fixed with respect to that reference frame. Since extragalactic sources (with the exception of 3C273) were not directly accessible for observation by Hipparcos, it was necessary to use other observational techniques to link the Hipparcos reference frame to the extragalactic frame. Since the Hipparcos and Tycho Catalogues are the first large-scale realisations of the ICRS in the optical domain, great importance was attached to the task of achieving this link to the best possible accuracy. This chapter describes the different techniques that were employed, the work done by the several groups contributing to the link, and how their results were combined in order to derive the reference frame finally adopted for the catalogues.

18.1. Motivation for the Link

Hipparcos was able to measure the angles between objects on its observing list very accurately. From these angles, and their variation in time, the positions and proper motions of the stars could be calculated in a single coordinate system covering the whole sky, and their absolute trigonometric parallaxes were obtained at the same time. However, because the angles between stars are invariant with respect to a rigid rotation of the coordinate axes, there was a basic indeterminacy in the instantaneous orientation of the axes that could not be removed from an analysis of the angular measurements alone. Given the kinematical constraint that stars in general have uniform space motions (as incorporated in the modelling of the observations; see Volume 1, Section 1.2.8), it can be shown that the intrinsic indeterminacy of the Hipparcos reference system has six degrees of freedom (Betti & Sansò 1983), corresponding to the inertial spin of the system and its orientation at a given epoch. More precisely, there is a six-dimensional manifold of solutions for the positions and proper motions, each solution being equally consistent with the observations and differing from the others by a uniform rotation. From this manifold of possible reference frames a single one had to be selected for the published catalogues. The selected reference frame should correspond to the International Celestial Reference System (ICRS), as discussed in Section 18.2.

The merging of the final FAST and NDAC sphere solutions, described in Chapter 17, resulted in a catalogue called H37C, the precise axes of which were in an unknown state

of uniform rotation with respect to the desired extragalactic frame. It was the purpose of the link observations to determine this state by all available means, and then apply the corresponding corrections to the positions and proper motions in H37C in order to produce the Hipparcos Catalogue.

A direct determination of the relation between H37C and the extragalactic system would have been possible if the Hipparcos observing programme had included a sufficient number of extragalactic sources, some of which with accurately known radio positions. However, due to the rather bright limiting magnitude of Hipparcos, no such objects were included. (The programme did include the brightest quasar, 3C273 (HIP 60936), and some 45 stars in the Magellanic Clouds; however, the quasar was still too faint to contribute significantly to the link, and the Magellanic Clouds are expected to have proper motions of a few milliarcsec per year, and therefore cannot be used as reference directions. See Section 18.8 for a discussion of the observations of these objects.) Consequently, indirect methods had to be used to bridge the gap between the optically bright objects on the observing list and the extragalactic sources observed either at radio wavelengths or at much fainter optical magnitudes. These methods and their results are described in subsequent sections. Since the actual orientation and spin of H37C found by these methods are only of historical interest (they are given in Table 16.8), while the deviations of the various methods from the adopted mean result are of considerable interest for judging the quality of the link, all results in this chapter are given relative the adopted mean result. Thus, the results of the individual link methods are presented as if the Hipparcos Catalogue (and not H37C) had been compared with the extragalactic frame.

18.2. Reference System for the Hipparcos Catalogue

The choice of a reference system for the Hipparcos Catalogue was initially not an obvious one. The traditional definition of the fundamental celestial directions in terms of the mean equator and equinox was based on dynamical principles and its practical implementation required observations both of solar system objects (to determine the ecliptic) and of the Earth's rotation axis (to determine the equator), as well as a dynamical theory for the inertial variations of these directions. However, it was clear from the outset that a kinematical definition of a non-rotating frame (i.e. with respect to distant galaxies) was much preferred for Hipparcos, because it would be both easier to implement and more accurate than a dynamical (inertial) system. This choice eliminated three degrees of freedom, but still left the orientation of the system unspecified. The situation was clarified in 1991, when the IAU adopted a resolution (Bergeron 1992) stating that the next celestial reference system should be based upon positions of extragalactic radio sources, but that it will come into effect only when there is a realisation of the system in the optical domain. It was then understood that this realisation should be the Hipparcos Catalogue, given its expected high precision and extension to more than a hundred thousand stars.

Since 1988, the International Earth Rotation Service (IERS) has implemented and maintained an extragalactic reference frame containing an increasing number of extragalactic radio sources observed by several VLBI networks throughout the world (Arias *et al.* 1995). At the request of the IAU working group on reference frames, IERS finalised this iterative process and provided a definitive list of objects and coordinates in October 1995 (Ma *et al.* 1997). This list is the International Celestial Reference Frame (ICRF)

of 610 sources (IERS 1996). The axes of this catalogue are to remain fixed with respect to the quasars, and constitute the International Celestial Reference System (ICRS). As a result of the present link, all the coordinates published in the Hipparcos and Tycho Catalogues refer to the ICRS. It is expected that in 1997 the IAU will approve ICRS as the new reference system replacing the FK5 system. The Hipparcos and Tycho Catalogues are its first realisation for optical astronomy.

18.3. Link Equations

The analytical tools for comparing two reference frames related by a uniform rigid-body rotation were derived in Lindegren & Kovalevsky (1995) and are summarised here to the extent that they are directly applicable to the various link observations.

The extragalactic reference frame (ICRF) is represented by the triad of unit vectors, $\mathcal{E} = [\,\mathbf{x}_\mathrm{E}\ \mathbf{y}_\mathrm{E}\ \mathbf{z}_\mathrm{E}\,]$. Similarly the Hipparcos reference frame is represented by the triad $\mathcal{H} = [\,\mathbf{x}_\mathrm{H}\ \mathbf{y}_\mathrm{H}\ \mathbf{z}_\mathrm{H}\,]$. Following the principle of coordinate transformations in Section 1.5.3 of Volume 1, the arbitrary direction $\mathbf{u}$ is written:

$$\mathbf{u} = \mathcal{E}\begin{pmatrix}\cos\delta_\mathrm{E}\cos\alpha_\mathrm{E}\\ \cos\delta_\mathrm{E}\sin\alpha_\mathrm{E}\\ \sin\delta_\mathrm{E}\end{pmatrix} = \mathcal{H}\begin{pmatrix}\cos\delta_\mathrm{H}\cos\alpha_\mathrm{H}\\ \cos\delta_\mathrm{H}\sin\alpha_\mathrm{H}\\ \sin\delta_\mathrm{H}\end{pmatrix} \qquad [18.1]$$

where $(\alpha_\mathrm{E}, \delta_\mathrm{E})$ and $(\alpha_\mathrm{H}, \delta_\mathrm{H})$ are the celestial coordinates of $\mathbf{u}$ in the two frames. The column matrices in Equation 18.1 containing the direction cosines can also be written $\mathcal{E}'\mathbf{u}$ and $\mathcal{H}'\mathbf{u}$, respectively. They are related through the matrix equation:

$$\mathcal{E}'\mathbf{u} = (\mathcal{E}'\mathcal{H})\,\mathcal{H}'\mathbf{u} \qquad [18.2]$$

where $\mathcal{E}'\mathcal{H}$ is an orthogonal 3×3 matrix whose elements consist of the scalar products $\mathbf{x}'_\mathrm{E}\mathbf{x}_\mathrm{H}$, etc.

The relation between $\mathcal{E}$ and $\mathcal{H}$ can be represented by the time dependent vector $\boldsymbol{\varepsilon}(T)$ such that a triad initially aligned with $\mathcal{H}$ will become aligned with $\mathcal{E}$ after rotation through the angle $\varepsilon = |\boldsymbol{\varepsilon}|$ about the unit vector $\mathbf{e} = \boldsymbol{\varepsilon}\varepsilon^{-1}$. In the small-angle approximation (neglecting terms of order ε^2) the frames are related by:

$$\mathcal{E} \simeq \mathcal{H} + \boldsymbol{\varepsilon}\times\mathcal{H} \qquad [18.3]$$

and the transformation matrix in Equation 18.2 becomes:

$$\mathcal{E}'\mathcal{H} \simeq \mathbf{I} + (\boldsymbol{\varepsilon}\times\mathcal{H})'\mathcal{H} = \begin{pmatrix}1 & \varepsilon_z & -\varepsilon_y\\ -\varepsilon_z & 1 & \varepsilon_x\\ \varepsilon_y & -\varepsilon_x & 1\end{pmatrix} \qquad [18.4]$$

Here, $\mathbf{I}$ is the 3×3 identity matrix and ε_x, ε_y, ε_z are the components of $\boldsymbol{\varepsilon}$ in either reference frame. (The actual orientation errors occurring in the link equations were less than 0.1 arcsec, so the small-angle approximation was always adequate. The rigorous expressions for arbitrarily large rotations are given in Lindegren & Kovalevsky 1995.) It can be noted that $\mathcal{E}'\boldsymbol{\varepsilon} = \mathcal{H}'\boldsymbol{\varepsilon}$ strictly holds, so that the components of the rotation vector are the same in the two frames.

If $\mathcal{H}$ is rotating with constant angular velocity $\boldsymbol{\omega}$ relative to $\mathcal{E}$, then its time dependent orientation error can be written (again in the small-angle approximation):

$$\boldsymbol{\varepsilon}(T) = \boldsymbol{\varepsilon}_0 + (T - T_0)\boldsymbol{\omega} \qquad [18.5]$$

where $\boldsymbol{\varepsilon}_0$ is the orientation error at the reference epoch T_0 = J1991.25. The link observations aim at the estimation of the six components of $\boldsymbol{\varepsilon}_0$ and $\boldsymbol{\omega}$ in the $\mathcal{E}$ or $\mathcal{H}$ frame, and the link equations express the observations in terms of these six unknowns, or a subset of them.

Positional Observations

Observations linking the positions of objects in the two frames provide information on the orientation difference $\boldsymbol{\varepsilon}$ at the (mean) epoch of observation, $T = T_0 + t$. Three kinds of positional link observations are considered here: (1) observation of the position of a Hipparcos star in the extragalactic frame; (2) observation of the position of an extragalactic object in the Hipparcos frame; and (3) measurement of the angular separation between two objects, one of which is known in the extragalactic frame, the other in the Hipparcos frame. Observations undertaken for each of these cases can be summarized as follows:

(1) Radio interferometric observations of a radio star allow its barycentric position $(\alpha_\mathrm{E}, \delta_\mathrm{E})$ in the extragalactic frame at the (mean) epoch T of the radio observations to be determined. (It can be assumed that the observations are corrected to the barycentre, using either the Hipparcos parallax or a parallax determined from the radio observations themselves.) Let $(\alpha_\mathrm{H}, \delta_\mathrm{H})$ be the barycentric position of this star at the same epoch T, as calculated from the position and proper motion data in the Hipparcos Catalogue. The two sets of celestial coordinates are related through Equations 18.1, 18.2 and 18.4. Neglecting terms of order $(\alpha_\mathrm{H} - \alpha_\mathrm{E})\varepsilon$ and $(\delta_\mathrm{H} - \delta_\mathrm{E})\varepsilon$ gives the following equations of condition:

$$\begin{pmatrix} -\sin\delta\cos\alpha & -\sin\delta\sin\alpha & \cos\delta \\ \sin\alpha & -\cos\alpha & 0 \end{pmatrix} \boldsymbol{\varepsilon}(T) = \begin{pmatrix} (\alpha_\mathrm{H} - \alpha_\mathrm{E})\cos\delta \\ \delta_\mathrm{H} - \delta_\mathrm{E} \end{pmatrix} \qquad [18.6]$$

The combination of several such observations spread over a number of years allows determination of $\boldsymbol{\varepsilon}_0$ and $\boldsymbol{\omega}$ separately by substituting Equation 18.5 in the left-hand side.

(2) Relative astrometric observations by means of photographic or CCD techniques, using Hipparcos stars as reference points, allow the position of an extragalactic object in the Hipparcos frame, $(\alpha_\mathrm{H}, \delta_\mathrm{H})$ to be determined. If its position $(\alpha_\mathrm{E}, \delta_\mathrm{E})$ in the extragalactic frame is also known, the same equations of condition result as in the previous case, Equation 18.6, where $T = T_0 + t$ is the epoch of the relative astrometric observation.

(3) Observations with the Hubble Space Telescope Fine Guidance Sensors allow the angular separation ϕ of two objects, e.g. between an extragalactic object (at $\mathbf{u}_1$) and a Hipparcos star (at $\mathbf{u}_2$) to be measured. The coordinates of the extragalactic object are known in the extragalactic frame ($\mathcal{E}'\mathbf{u}_1$), while those of the Hipparcos star are known in the Hipparcos frame ($\mathcal{H}'\mathbf{u}_2$). This type of observation differs from the previous two in that none of the objects is accurately known in both frames. The following implicit form of link equation is readily obtained by means of Equations 18.2 and 18.4:

$$\begin{aligned} 2\sin\frac{\phi}{2} &= |\mathbf{u}_1 - \mathbf{u}_2| = |\mathcal{E}'\mathbf{u}_1 - \mathcal{E}'\mathbf{u}_2| = |\mathcal{E}'\mathbf{u}_1 - (\mathcal{E}'\mathcal{H})\mathcal{H}'\mathbf{u}_2| \\ &= \left| \begin{pmatrix} \cos\delta_{\mathrm{E}1}\cos\alpha_{\mathrm{E}1} \\ \cos\delta_{\mathrm{E}1}\sin\alpha_{\mathrm{E}1} \\ \sin\delta_{\mathrm{E}1} \end{pmatrix} - \begin{pmatrix} 1 & \varepsilon_z & -\varepsilon_y \\ -\varepsilon_z & 1 & \varepsilon_x \\ \varepsilon_y & -\varepsilon_x & 1 \end{pmatrix} \begin{pmatrix} \cos\delta_{\mathrm{H}2}\cos\alpha_{\mathrm{H}2} \\ \cos\delta_{\mathrm{H}2}\sin\alpha_{\mathrm{H}2} \\ \sin\delta_{\mathrm{H}2} \end{pmatrix} \right| \end{aligned} \qquad [18.7]$$

An explicit form can be obtained by linearisation.

Proper Motions

Let $(\mu_{\alpha*\mathrm{H}}, \mu_{\delta\mathrm{H}})$ and $(\mu_{\alpha*\mathrm{E}}, \mu_{\delta\mathrm{E}})$ be the proper motion components of one and the same object, expressed in the Hipparcos and extragalactic frames. Their differences give directly an observation equation for the spin difference:

$$\begin{pmatrix} -\sin\delta\cos\alpha & -\sin\delta\sin\alpha & \cos\delta \\ \sin\alpha & -\cos\alpha & 0 \end{pmatrix} \boldsymbol{\omega} = \begin{pmatrix} \mu_{\alpha*\mathrm{H}} - \mu_{\alpha*\mathrm{E}} \\ \mu_{\delta\mathrm{H}} - \mu_{\delta\mathrm{E}} \end{pmatrix} \qquad [18.8]$$

Stellar proper motions in the Hipparcos frame are known from the space observations. The proper motions of some of these stars were also known in the extragalactic frame, either from VLBI observations (in the case of radio stars), or from photographic surveys determining 'absolute' stellar proper motions with respect to background galaxies. A third kind of observations leading to the same form of link equation is the measurement of the apparent proper motions of sufficiently distant extragalactic objects in the Hipparcos reference frame; in this case $\mu_{\alpha*\mathrm{E}} = \mu_{\delta\mathrm{E}} = 0$ is assumed.

Use of Earth Orientation Parameters

The Earth Orientation Parameters (EOP) are a set of time dependent angles describing the orientation of the Earth's spin axis and the phase of the spin about the axis. The spin axis orientation is given in the terrestrial system by the two components of the polar motion (denoted x, y), and in the celestial system by the offsets in obliquity ($\Delta\epsilon$) and longitude ($\Delta\psi \sin\epsilon$) of the nutation angles from a conventional model of precession and nutation. The instantaneous phase of the spin is given by universal time (UT1), and the corresponding Earth orientation parameters set is taken to be its offset from the international atomic time scale, UT1–TAI. Since 1980 these angles are derived with sub-milliarcsec accuracy from VLBI observations relative to extragalactic radio sources in the IERS reference system. The celestial orientation of the Earth, given by $\Delta\epsilon$, $\Delta\psi \sin\epsilon$ and UT1–TAI, are thus accurately known in the extragalactic reference system.

But the Earth orientation parameters can also be derived from latitude and time observations obtained by optical instruments, typically zenith tubes and astrolabes. Indeed, this was the standard method before the advent of radio interferometry. In this case the celestial orientation of the Earth is determined with respect to the optical reference system of the stars used in the observations. Clearly a comparison of the Earth orientation parameters as derived by VLBI and by the traditional optical means provides an indirect link between the two reference systems. In terms of the orientation vector $\boldsymbol{\varepsilon}$ at the epoch of observation, the link equations are:

$$\begin{aligned} \varepsilon_x &= -(\Delta\epsilon_{\mathrm{H}} - \Delta\epsilon_{\mathrm{E}}) \\ \varepsilon_y &= (\Delta\psi_{\mathrm{H}} - \Delta\psi_{\mathrm{E}})\cos\epsilon \\ \varepsilon_z + \Delta\lambda &= 15\,041(\mathrm{UT1}_{\mathrm{H}} - \mathrm{UT1}_{\mathrm{E}}) \end{aligned} \qquad [18.9]$$

where $\epsilon \simeq 23^\circ\!.44$ is the obliquity of the ecliptic and $\Delta\lambda$ is the longitude difference between the two realisations of the terrestrial system. The numerical factor 15 041 converts seconds of Universal Time to mas. Unfortunately $\Delta\lambda$ is essentially unknown, at the accuracy level of interest here, and the Earth orientation parameters method can therefore only be used to determine the x and y components of the link. The time-dependent part of Equation 18.9 gives the observation equations for $\boldsymbol{\omega}$. Assuming that

$\Delta\lambda$ is constant, it should be possible to obtain all three components of $\boldsymbol{\omega}$ from these equations; however, the actual results indicate that there is also a drift in $\Delta\lambda$, so that only ω_x and ω_y can be determined.

18.4. Results of the Different Link Programmes

In the following subsections, the various programmes used for the determination of the extragalactic link are described individually. The participants of each group are listed in Section 18.9. The link programmes are presented in the following order:

1. radio and optical techniques providing high-precision positional links to a small number of Hipparcos stars. These define the orientation parameters $\boldsymbol{\varepsilon}$ very accurately, but contribute less to the determination of the spin ($\boldsymbol{\omega}$) due to the small number of objects and the relatively short time span of the observations;
2. use of proper motion surveys where the motions of large numbers of stars are measured relative to galaxies. These only contribute to the determination of $\boldsymbol{\omega}$;
3. special photographic link programmes;
4. use of Earth orientation parameters.

The numerical results of the individual link solutions, expressed as residuals with respect to the adopted global solutions, are given in Tables 18.3–18.4. Further details on the individual solutions are found in Kovalevsky *et al.* (1997) and in separate papers prepared by the different groups.

VLBI Observations

Multi-epoch VLBI observations were conducted between 1984 and 1994 to determine the positions, proper motions and parallaxes of 12 radio-emitting stars. Their positions on the sky are shown in Figure 18.1. The observations were conducted on the US VLBI Network, NASA Deep Space Network, NRAO Very Large Baseline Array (VLBA) and European VLBI Network. The data processing and analysis is described in Lestrade *et al.* (1995). All the VLBI observations for each star were phase-referenced to an angularly nearby extragalactic radio source on the ICRF list. The resulting uncertainties in the astrometric parameters of the radio stars are presented in Table 18.1. The parallax results are discussed in Section 20.3.

The six components of $\boldsymbol{\varepsilon}_0$ and $\boldsymbol{\omega}$ were simultaneously solved by a least-squares fit as described in Lestrade *et al.* (1995), using weights based on the combined VLBI and Hipparcos *a priori* measurement uncertainties. Two objects were however down-weighted by increasing their positional uncertainties by a factor of three: for HIP 12469 (LSI 61°303) because of its jet structure on a 10 mas scale, and for HIP 19762 (HD 283447) because of its known duplicity on a scale $\simeq$ 0.1 arcsec (Ghez *et al.* 1993) which is difficult for Hipparcos. No modifications were made on the *a priori* proper motion uncertainties. After this adjustment of the weights, the unit-weight residual of the solution was close to unity.

Tests were done by splitting the 12 stars in various subsets and calculating independent solutions for each subset. This showed that the fit is quite robust: for instance, the

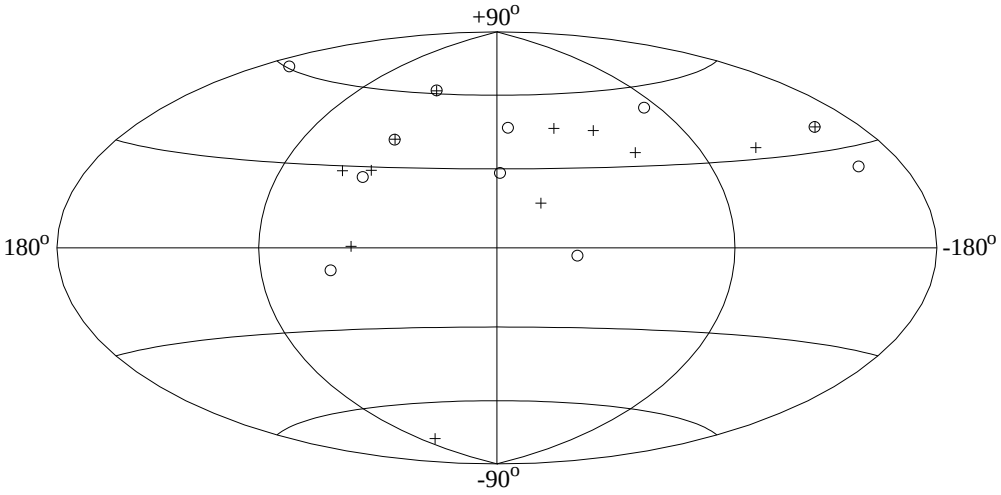

Figure 18.1. *Sky distribution of radio stars used for the link by VLBI (crosses) and MERLIN (circles). Equatorial projection with α increasing from -180° to $+180^\circ$ right-to-left.*

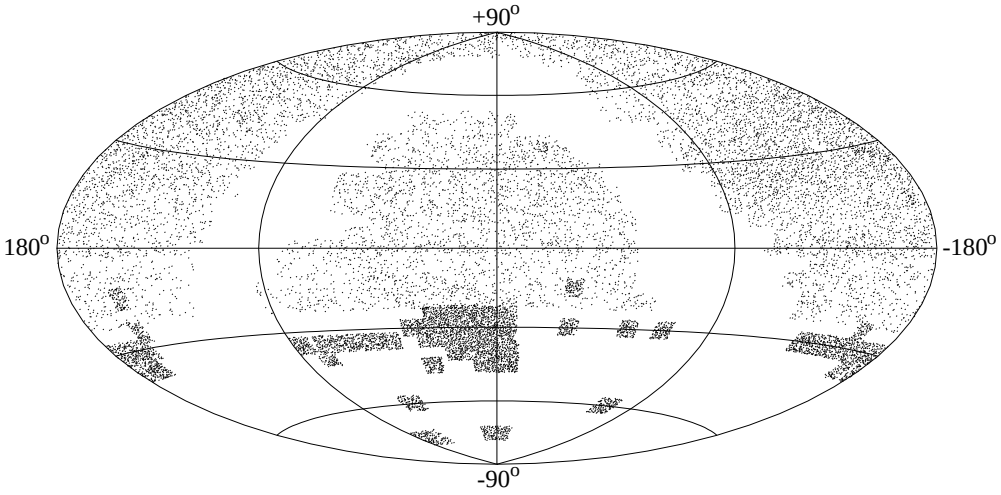

Figure 18.2. *Sky distribution of Lick NPM1 fields (light grey) and Yale/San Juan SPM fields (dark grey) used in the link solutions. Equatorial projection with α increasing from -180° to $+180^\circ$ right-to-left.*

Table 18.1. Uncertainties of the absolute positions (at epoch J1991.25), proper motions and trigonometric parallaxes of the 12 link stars as determined by VLBI observations.

Hipparcos number (HIP)	Star name	Standard errors Pos. (mas)	P.M. (mas/yr)	Par. (mas)
12469	LSI 61°303 = V615 Cas	3.0	0.30	0.62
14576	Algol	0.61	0.18	0.59
16042	UX Ari	2.1	0.20	0.39
16846	HR 1099	0.48	0.31	0.47
19762	HD 283447	3.0	0.28	0.25
23106	HD 32918	1.5	1.00	0.80
66257	HR 5110	1.28	0.16	0.45
79607	σ^2 CrB	0.29	0.05	0.10
98298	Cyg X1 = V1357 Cyg	1.50	0.14	0.30
103144	HD 199178	1.95	0.43	0.33
109303	AR Lac	0.94	0.19	0.37
112997	IM Peg	1.42	0.47	0.68

differences between the fits of two subsets of six stars each were within the combined uncertainties, i.e. less than 1 mas for the orientation components and less than 0.6 mas/yr for the spin components.

Observations with MERLIN

MERLIN is a real-time radio-linked radio interferometer array with a maximum baseline of 217 km, giving a resolution of approximately 40 mas at 5 GHz. See Thomasson (1986) for a general description of MERLIN. As in the VLBI observations described above, the positions of weak radio stars were obtained by using ICRF sources as phase calibrators. Typically, the star-calibrator separation was 5° and the cycle time was 5 to 10 min.

A total of 13 radio stars were observed between 1992 and 1995, four of which are common with the VLBI set: HIP 12469 (LSI 61°303), HIP 14576 (Algol), HIP 16879 (HD 22403), HIP 19431 (HD 26337), HIP 53425 (DM UMa), HIP 65915 (FK Com), HIP 66257 (HR 5110), HIP 79607 (σ^2 CrB), HIP 85852 (29 Dra), HIP 91009 (BY Dra), HIP 108644 (FF Aqr), HIP 116584 (λ And), and HIP 117915 (II Peg). The positions of individual stars, relative to the ICRF sources, are estimated to have individual errors of approximately 4 mas. Two of the stars (HIP 85852 and HIP 79607) were not included in the link solution because of problems related to the duplicity of these objects. The distribution of the retained stars on the sky is shown in Figure 18.1.

The Hipparcos proper motions and parallaxes were used to reduce the MERLIN geocentric positions to the barycentre and mean epoch of Hipparcos, i.e. J1991.25. For the triple star Algol, a further correction from the radio emitting close pair AB to the centre of mass of the AB–C system was applied, using the orbital elements and mass ratios by Pan *et al.* (1993). Compared with that reference, however, the position angle of the line of nodes had to be rotated by 180° to obtain agreement with the MERLIN data.

The solution for $\boldsymbol{\varepsilon}$ (at the mean epoch J1994.0) gives standard errors of 2.2 to 2.6 mas in the components. Compared with the VLBI solution which is virtually independent, there is a close agreement which lends confidence to the stability of the link which could have been distorted by significant offsets between the optical and radio emission of some of the binary stars.

Observations with the VLA

As part of the link programme, observations were also carried out with the Very Large Array (VLA) operated by the National Radio Astronomy Observatory. For this observing programme the procedures outlined in Florkowski *et al.* (1985) were followed. Between March 1982 and August 1995, radio emitting stars were observed differentially with respect to unresolved extragalactic radio sources. Cleaned maps of the sky near the stellar radio emission were created using the Astronomical Image Processing System (AIPS). The position of the star relative to the absolute phase centre of the map was obtained by fitting a two-dimensional Gaussian function to the stellar emission. The stellar positions (in the extragalactic reference frame) were moved to the epoch J1991.25 by means of the Hipparcos proper motions and parallaxes. The differences between the radio and Hipparcos positions were then used to solve for the orientation vector $\boldsymbol{\varepsilon}$ at the mean epoch of observation (around 1986). The standard error in each component of the vector was about 5 mas.

Optical Positions of Compact Sources

The Hamburg/USNO reference frame programme has been described in Johnston *et al.* (1995), Ma *et al.* (1990), and Zacharias & de Vegt (1995), and the reader is referred to these publications for details. The programme is aimed at the determination of precise optical and radio positions of about 400 to 500 selected compact radio sources which display optical counterparts, mostly QSOs and BL Lac's, within a visual magnitude range of 12 to 21 mag. Optical positions in the Hipparcos reference frame were obtained via a system of secondary reference stars in the magnitude range 12 to 14 mag. The procedure thus required two steps: first the establishment of the secondary reference positions by means of astrograph plates, and then the observation of the radio sources with respect to the secondary frame by means of larger telescopes.

The secondary frame was established using wide field ($\simeq 5°$) astrographs on both hemispheres. For each field, four plates centred on the source position were taken and measured on the CCD-camera based Hamburg astrometric measuring machine. The measurements included all Hipparcos stars in the whole plate field (typically 50 to 100 stars), and secondary reference stars selected from the Hubble Space Telescope Guide Star Catalog in the central 1° field. Formally, the Hipparcos reference frame could be transferred locally to each radio source field with a precision better than 10 mas.

Optical source positions were then obtained using plates from Schmidt telescopes and the prime focus of large telescopes. Plate or CCD solutions were obtained using the secondary reference star catalogue. The precision of the optical source positions based on several plates and/or CCD frames is better than 30 mas in each case. The programme therefore provides optical positions of the extragalactic reference frame sources in the Hipparcos frame. The link solution used here was based on the CCD frames of 78 globally selected sources at mean epoch J1988.5 and gives a formal error of about 5 mas in each component of the orientation vector at that epoch. The full programme will

eventually determine the orientation parameters on the 1 mas accuracy level, based on all 400 sources.

Observations with the Hubble Space Telescope

The Fine Guidance Sensors (FGSs) of the Hubble Space Telescope (HST) have been used to measure the angular separation of Hipparcos stars from extragalactic objects. Within the instrumental frame the FGSs measure relative positions of targets to a precision of a few milliarcsec (Benedict *et al.* 1992). However, since the absolute orientation of the FGS frames is not accurately known, the relative positions in the FGS field of view cannot be transformed to differences in α and δ on the sky. The angular separation of two objects, being independent of the FGS orientation, is therefore the most accurate datum available for the link work.

78 separations of 46 Hipparcos stars next to 34 extragalactic objects were measured from April 1993 through December 1995. GaussFit, a non-linear least-squares package (Jefferys *et al.* 1988), was used to determine the orientation and spin parameters from these data. The Hipparcos proper motion and parallax values were used to calculate the topocentric directions of the stars at the times of observation. The analysis required the application of a time-dependent field distortion calibration and the inclusion of a time-dependent scale factor among the fitted parameters. The major sources of error are the HST/FGS data (estimated at 3 to 4 mas for a single separation measurement) and the propagation of the Hipparcos proper motion errors to the epochs of the HST observations.

Use of the Lick Proper Motion Program

The published Part 1 of the Lick Observatory Northern Proper Motion Program (NPM), also known as NPM1 (Klemola *et al.* 1987, 1993, 1994), contains 149 000 stars from 899 NPM fields north of $\delta = -23°$ for which the proper motions have been determined relative to background galaxies. The mean number of galaxies per field is 80. The typical precision of the NPM1 absolute proper motions is 5 mas/yr.

In total 13 455 stars are common to the NPM1 catalogue and the Hipparcos Catalogue. Preliminary comparisons of Hipparcos proper motions with the NPM1 indicated a linear magnitude equation of about 1 mas yr^{-1} mag^{-1} in the NPM1 data essentially down to the magnitude limit of the Hipparcos Catalogue. The magnitude equation is coordinate-independent, although in declination it shows a different slope for stars north and south of $\delta = -2\overset{\circ}{.}5$. It should be noted that due to the lack of measurable multiple grating images in the same exposure, it is impossible to eliminate the magnitude equation internally. Furthermore, there are no absolute proper motions available which could readily be used to correct the magnitude equation externally. Since the rotation parameters are correlated with the magnitude equation, the Hipparcos data cannot be used to correct the magnitude equation as part of the link solution.

Two different groups have independently analysed the Hipparcos–NPM1 differences in an attempt to contribute to the extragalactic link of the Hipparcos Catalogue. Their conclusions are separately reported below.

The Yale Analysis: With regard to the magnitude equation described above, affecting the bright NPM1 stars, various solutions to the problem were tried, including the

Table 18.2. Results of the Heidelberg solutions for the components of the spin vector $\boldsymbol{\omega}$ (in mas/yr) using the Lick NPM1 proper motions. The first line gives the solution without magnitude limits for the selection of stars; subsequent lines give the results for stars in certain intervals of the Lick (m_B) or Hipparcos (Hp) magnitude. The last line gives the formal standard errors for the solution with 1135 stars.

Magnitude range	Number of stars	Spin components ω_x	ω_y	ω_z
(no limit)	9236	−0.70	−0.27	−2.14
$10.5 < m_B < 11.5$	2616	−0.76	+0.17	−0.85
$10.9 < m_B$	2220	−0.72	+0.02	+0.10
$11.9 < m_B$	510	−0.25	−0.12	+0.84
$10.0 < Hp < 12.2$	2535	−0.81	+0.11	−0.25
$10.6 < Hp < 12.2$	1135	−0.85	+0.16	+0.60
Formal errors:	1135	0.25	0.20	0.20

use of additional parameters in the link equations corresponding to linear magnitude equations in each coordinate. Unambiguous disentangling of the magnitude effect from the spin parameters turns out to be very difficult and perhaps impossible, due to the strong correlations among these parameters. A careful inspection of how the magnitude equation affects the spin components indicates the significance of the star distribution over the sky. One possibility of minimising the effect of a coordinate-independent magnitude equation is to seek a well-balanced distribution of the stars. In other words, for the spin components ω_x and ω_y the stars must be distributed such that the sums of the corresponding geometrical weighting factors in Equation 18.8 are close to zero. In practice, the distribution of the NPM1 stars used in the solution was balanced by introducing a fictitious 44°-width 'zone of avoidance' perpendicular to the galactic plane. In addition, the stars with $\delta < -2\overset{\circ}{.}5$ (only in the declination solution) and $m_B < 10$ mag were deleted from the sample in order to reduce further the effect of the magnitude equation. Four different solutions were computed from images of different colours (blue, visual) and components (α, δ).

The Heidelberg Analysis: In order to investigate a possible magnitude equation in the Lick data, spin solutions were computed for stellar samples of different brightness (Table 18.2). It turned out that the dependence on magnitude is relatively unimportant for ω_x and ω_y. (The case of $m_B > 11.9$ mag was not considered representative, because of the small number of stars in that sample.) ω_z, on the other hand, shows a strong dependence on magnitude. Moreover, there seems to be no asymptotic behaviour when going to fainter stars. The conclusion is that ω_z cannot be reliably determined from the Lick proper motions. These findings are confirmed by Hanson (1996, private communication) who reported on small systematic errors in the Lick proper motions in right ascension.

Catalogue of Faint Stars (KSZ)

A general catalogue of absolute proper motions of stars with respect to galaxies was compiled by Rybka & Yatsenko (1996), using data from 185 sky areas produced in Kiev, Moscow, Pulkovo, Shanghai and Tashkent. The catalogue includes 977 Hipparcos stars in the magnitude range 4 to 13 mag.

Proper motion differences were analysed according to Equation 18.8. The residuals in each coordinate were analysed as functions of magnitude, colour and position on the sky. No significant dependency on these variables was found: the residuals represent random errors only. However, different results for $\boldsymbol{\omega}$ were obtained when the whole interval of stellar magnitudes was used and when only bright (≤ 9.0 mag) or faint (> 9.0 mag) stars were used. Since the stellar data in KSZ were obtained relative to faint galaxies it was assumed that the solution using only the fainter stars is the more reliable one for the link. For that solution, 415 stars were kept from 154 areas of the sky, yielding standard errors of about 0.8 mas/yr for the spin components.

The Yale/San Juan Southern Proper Motion Program

The Yale/San Juan Southern Proper Motion program (SPM) is an extension of the Lick Observatory Northern Proper Motion program to the sky south of $\delta = -17°$. A brief description of the observational material can be found in van Altena *et al.* (1990) and Platais *et al.* (1995). In total 63 SPM fields, containing about 4100 Hipparcos stars, were measured and reduced for the Hipparcos link (Figure 18.2). The mean number of reference galaxies per field is 250 on blue plates and 190 on visual plates, yielding a mean uncertainty in the correction to absolute proper motions of 1.0 mas/yr for each field. Since the Hipparcos stars are represented by several images per star (ten in the most favourable case), the single proper motion precision in each colour (blue or visual) can be as good as 2 to 3 mas/yr. If this error were composed entirely by the random measurement and modelling errors, the precision of each spin component with the given number of the Hipparcos stars in hand could be in the range of 0.1 to 0.2 mas/yr. However, the link solutions indicate a somewhat larger scatter in the spin components when compared to this precision estimate. This may very well be due to a small systematic error remaining after the correction for the magnitude equation.

A preliminary study of the systematic errors in the SPM plates (Platais *et al.* 1995) clearly showed the presence of a significant magnitude equation in the SPM coordinates. The bulk of the magnitude equation in coordinates and, presumably, in proper motions was removed using the grating-image offset technique formulated by Jefferys (1962) and modified by the present group. This technique has inherent limitations set by the small number of stars at the bright end, and by the fact that the magnitude equation may have a complicated form, too difficult to model adequately. In addition, the magnitude equation in the SPM plates is stronger and more complex in declination than in right ascension. It was therefore believed that the link solution using only the proper motions in right ascension was less affected by systematic errors related to the magnitude effect.

The Bonn Link Solution

The Bonn link solution uses series of photographic plates characterised by very large epoch differences, typically 70 years and up to 100 years (Brosche *et al.* 1991). Each series contains a compact extragalactic source and several Hipparcos stars, from which the (apparent) proper motion of the extragalactic object in the Hipparcos frame can be derived. The plates were predominantly taken with the $f = 5$ m double refractor of the Sternwarte Bonn. For some fields the relative proper motions were calibrated using a large number of stars and galaxies on Schmidt plates and Lick astrographic plates.

The link solution used 88 Hipparcos stars in 13 fields distributed over the northern celestial hemisphere. The median uncertainty for each field was 1.3 mas/yr. No significant correlations of the residuals from this solution with magnitude, colour, spherical coordinates or relative position within a field were found.

The Potsdam Link Solution

The Potsdam programme (Dick *et al.* 1987) is based on measurements of plates (using MAMA and APM) taken with the Tautenburg Schmidt telescope (134/200/400 cm). Proper motions of 360 Hipparcos stars were derived in 24 fields (each of about 10 square degrees) well distributed over the northern sky. From 200 to 2000 galaxies per field were used to link the proper motions to the extragalactic reference system. With at least two plate pairs per field and epoch differences of 20 to 40 years, an internal precision of 3 to 5 mas/yr was achieved for the proper motions of Hipparcos stars (Kharchenko *et al.* 1994). Due to the large number of galaxies in each field the formal zero point error is less than 1 mas/yr.

Previous investigations showed that systematic, magnitude-dependent errors could affect the proper motions of bright stars measured on Tautenburg plates (Scholz & Kharchenko 1994, Kharchenko & Schilbach 1995). A significant magnitude equation was indeed found by comparison with the bright Hipparcos stars. To minimise the effect, only 256 Hipparcos stars fainter than $m_B = 9.0$ mag were used for the link, yielding formal errors of 0.5 mas/yr on the components of $\boldsymbol{\omega}$. The rms residual in the proper motions of stars was 6.9 mas/yr.

Use of Earth Orientation Parameters

VLBI determines the five Earth orientation parameters $\Delta\epsilon$, $\Delta\psi \sin\epsilon$, UT1–TAI, x and y, in the extragalactic frame, at roughly 5-day intervals. The same parameters, referred to the celestial optical system tied to the stars of the Galaxy, can be determined by optical astrometry following the algorithms outlined in Vondrák (1991, 1996) and Vondrák *et al.* (1992, 1995). Using the preliminary Hipparcos Catalogue, all the latitude and UT observations made with 46 instruments at 29 different observatories all over the world were recalculated into that reference frame. About 3.6 million observations were used to derive Earth orientation parameters at 5-day intervals between 1899.7 and 1992.0. However, only the last twelve years in common with the VLBI observations were actually used for the link. Moreover, only the first two components of the orientation vector $\boldsymbol{\epsilon}$ were determined, for the reasons explained in Section 18.3.

Summary of Numerical Results

The results of the individual link solutions are summarised in Tables 18.3–18.4 and presented graphically in Figures 18.3–18.4. The galactic x and y components of the solutions are also shown in Figures 18.5–18.6. As previously explained, the results given in these tables and figures are the residuals of the individual solutions with respect to the adopted solution found by the synthesis described in Section 18.7. For the orientation components the residuals refer to the approximate mean epoch of observation of the link observations in question given in the last column of Table 18.3.

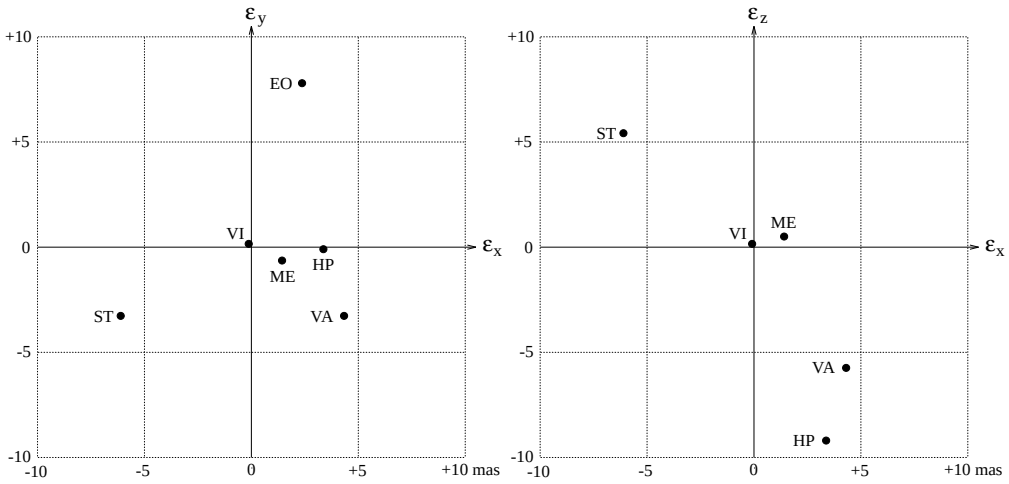

Figure 18.3. *Projections onto the xy and xz planes of the individual solutions for the orientation vector* $\boldsymbol{\varepsilon}$ *(residuals with respect to the adopted vector at the mean epoch of each solution). The components are expressed in mas. The solutions are labelled as in Table 18.3. See also Figure 18.5 for the projections onto the galactic xy plane.*

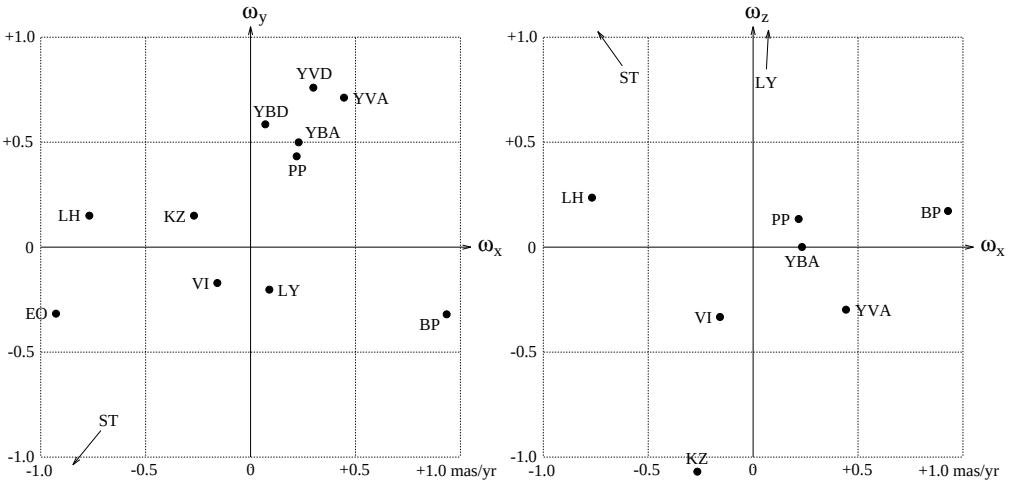

Figure 18.4. *Projections onto the xy and xz planes of the individual solutions for the spin vector* $\boldsymbol{\omega}$ *(actually residuals with respect to the adopted vector). The components are expressed in mas/yr. The solutions are labelled as in Table 18.4. See also Figure 18.6 for the projections onto the galactic xy plane.*

Table 18.3. Results of the individual link solutions for the orientation vector $\boldsymbol{\varepsilon}$, expressed as residuals with respect to the adopted solution. The second column contains the abbreviations used to identify the solutions in Figure 18.3. The (formal) standard errors supplied with the individual solutions are given in parentheses. The last column gives the approximate mean epoch of the link observations used to determine the orientation.

Method	Label	Orientation components (mas)			Epoch
		ε_X	ε_Y	ε_Z	1900+
VLBI	VI	−0.10 (0.47)	+0.08 (0.49)	+0.16 (0.50)	91.3
MERLIN	ME	+1.41 (2.60)	−0.64 (2.20)	+0.51 (2.40)	94.0
VLA	VA	+4.27 (4.70)	−3.75 (5.30)	−5.76 (5.20)	86.3
Hamburg/USNO	HP	+3.38 (5.00)	−0.06 (4.90)	−9.20 (4.70)	88.5
HST/FGS	ST	−6.10 (2.16)	−3.25 (1.49)	+5.42 (2.14)	94.3
EOP	EO	+2.33 (0.88)	+7.80 (0.90)		85.0

Table 18.4. Results of the individual link solutions for the spin vector $\boldsymbol{\omega}$, expressed as residuals with respect to the adopted solution. The second column contains the abbreviations used to identify the solutions in Figure 18.4. The (formal) standard errors supplied with the individual solutions are given in parentheses. The components marked with an asterisk (*) were not used in the synthesis.

Method	Label	Spin components (mas/yr)		
		ω_X	ω_Y	ω_Z
VLBI	VI	−0.16 (0.30)	−0.17 (0.26)	−0.33 (0.30)
HST/FGS	ST	−1.60 (2.87)	−1.92 (1.54)	+2.26 (3.42)
NPM (Heidelberg)	LH	−0.77 (0.40)	+0.15 (0.40)	+0.23 (*)
NPM (Yale)	LY	+0.09 (0.18)	−0.20 (0.18)	+1.46 (*)
KSZ Kiev	KZ	−0.27 (0.80)	+0.15 (0.60)	−1.07 (0.80)
SPM (blue, α)	YBA	+0.23 (0.13)	+0.50 (0.20)	0.00 (0.08)
SPM (blue, δ)	YBD	+0.07 (0.15)	+0.58 (0.08)	
SPM (visual, α)	YVA	+0.44 (0.12)	+0.71 (0.18)	−0.30 (0.07)
SPM (visual, δ)	YVD	+0.30 (0.12)	+0.76 (0.06)	
Bonn plates	BP	+0.93 (0.34)	−0.32 (0.25)	+0.17 (0.33)
Potsdam plates	PP	+0.22 (0.52)	+0.43 (0.50)	+0.13 (0.48)
EOP	EO	−0.93 (0.28)	−0.32 (0.28)	

18.5. Discussion of the Individual Solutions

Before describing the methods and results of the synthesis, some remarks should be made on the data provided by the various link techniques.

Radio Techniques

The relative precisions provided by the three interferometric techniques in the determination of the orientation (ε) are consistent with their baseline lengths and are therefore considered as realistic. The precision of the determination of the spin (ω) depends both on the basic uncertainty of the observations and on the time span. This gives a major advantage to the VLBI observations both for the orientation and spin. An attempt was made to determine ω with MERLIN observations, but the result was not retained, the time span being notably insufficient. A major concern with the radio techniques was the small number of link objects and the consequently rather high sensitivity of the solution to possible offsets of the radio and optical centres of emission. It was therefore very important to support these techniques by independent optical links to other extragalactic sources.

Optical Determination of the Orientation

The full Hamburg/USNO programme comprises some 400 extragalactic sources, but only about 20 per cent were completed at the time of the link. The Hubble Space Telescope observations started very late due to the well known problems with the telescope. In both cases, the uncertainties are large, but the methods are promising and would have given better results with more data. Nevertheless, the results obtained are in acceptable agreement with the radio techniques and support the adopted link within the uncertainties of the optical techniques, namely a few milliarcsec.

Photographic Catalogues Referred to Galaxies

These techniques are much more sensitive to magnitude-dependent errors than the preceding two optical methods. Most of the stars measured in these surveys are faint and comparable in magnitude with the reference galaxies. However, for the link one had to choose only the brightest of the survey stars, for which the effect is likely to be much larger. The magnitude dependence is not necessarily linear at this end of the survey population and the link results depend strongly upon either the model applied or the magnitude cut-off adopted. This is illustrated by the discussions of the NPM, SPM and KSZ programmes in the preceding section. No result can be considered as being unbiased in this respect, although the SPM solutions have an advantage in that the magnitude equation could be calibrated internally by the grating image technique.

The formal errors given by the authors of these methods are small because of the large number of stars, and cannot be considered as realistic. Additional biases related to the magnitude, and perhaps to other factors less well studied, certainly exist. This has justified a significant down-weighting of the results provided. The difference between

the results obtained at Yale and Heidelberg in their analyses of the NPM1 stars also justifies this policy.

Special Photographic Link Programmes

Relying on archival plates for the first-epoch measurements, these programmes are also prone to magnitude equation, with little possibility of controlling or studying the effect. Because of this, their formal errors are probably underestimated. Strangely enough, there seems to have been little gain in having a very long time span. Possibly the magnitude-dependent errors are larger or more difficult to model in the old plates, offsetting the advantage of the long time baseline.

Earth Orientation Parameters

In a sense this method is less direct than the others, as it depends on an intermediate (terrestrial) reference frame, whose relations in the optical and radio domain may not be completely understood. Apart from the problem with the z components discussed in the preceding section, an additional uncertainty arises from the fact that the mean epoch of the observations is 1985 and that all were performed before the Hipparcos mean epoch. In the synthesis method where only $\boldsymbol{\varepsilon}_0$ was estimated, this led to a considerable down-weighting of the data. However, even when the strong correlation between $\boldsymbol{\varepsilon}_0$ and $\boldsymbol{\omega}$ was taken into account, the formal errors had to be substantially increased to make sense in relation to other data.

18.6. Synthesis of the Link Solutions: General Methods

The synthesis of the individual link solutions was made independently by L. Lindegren and J. Kovalevsky, using methods (referred to as Method A and Method B below) which differ not only in implementation but also in the detailed treatment of the orientation and spin components and in the weighting of the individual solutions.

Method A

This method is described in detail in Lindegren & Kovalevsky (1995) and was strictly followed. As shown in that paper, it is possible to cast the results of each individual link solution (j) in the form of an information array $[\,\mathbf{N}_j \;\; \mathbf{h}_j\,]$ representing the normal equations $\mathbf{N}_j\mathbf{s} = \mathbf{h}_j$ for the six-dimensional state vector $\mathbf{s} = [\,\varepsilon_{0x}\;\varepsilon_{0y}\;\varepsilon_{0y}\;\omega_x\;\omega_y\;\omega_y\,]'$. The symmetric 6×6 matrix $\mathbf{N}_j$ has full rank only for the techniques providing an estimate of all six components of the state vector, which is then given by the solution $\mathbf{s}_j = \mathbf{N}_j^{-1}\mathbf{h}_j$ together with its formal covariance matrix $\mathbf{N}_j^{-1}$. Other link solutions providing only partial information on the state vector can still be expressed as an information array $[\,\mathbf{N}_j \;\; \mathbf{h}_j\,]$, but $\mathbf{N}_j$ is then singular, with $r_j = \mathrm{rank}(\mathbf{N}_j) < 6$ being the number of state vector components determined. In setting up the information arrays, the full set of correlations among the determined parameters were taken into account; in particular the correlations between the orientation and spin components were important for a uniform treatment of the different mean observation epochs shown in Table 18.3.

The individual link solutions $j = 1 \ldots J$ were given *a posteriori* weight factors $0 < w_j \leq 1$ according to a semi-automatic procedure described below. This corresponds to a set of multiplicative factors $w_j^{-1/2} \geq 1$ on the formal standard errors provided by the link groups. The weighted synthesis solution is then given by:

$$\hat{\mathbf{s}} = \left(\sum_{j=1}^{J} w_j \mathbf{N}_j \right)^{-1} \sum_{j=1}^{J} w_j \mathbf{h}_j \qquad [18.10]$$

where the inverse matrix also provides the estimated covariance of $\hat{\mathbf{s}}$.

The main problem is to assign the weight factors w_j. This must be done in such a way that the distances of the individual link solutions from $\hat{\mathbf{s}}$ are compatible with the (re-weighted) standard errors, taking into account the correlations among the components of the individual solutions $\mathbf{s}_j$ and the synthesised solution. This is complicated by the fact that only few of the link techniques provide an estimate of the full state vector. In practice a goodness-of-fit of each solution was computed from the re-weighted residual vector of the normal equations:

$$\mathbf{d}_j = w_j(\mathbf{h}_j - \mathbf{N}_j \hat{\mathbf{s}}) \qquad [18.11]$$

Assuming that $w_j \mathbf{N}_j$ is the correct information matrix for estimate j, the expected covariance of $\mathbf{d}_j$ is then given by:

$$\mathbf{D}_j = w_j \mathbf{N}_j - w_j \mathbf{N}_j \left(\sum_{j=1}^{J} w_j \mathbf{N}_j \right)^{-1} w_j \mathbf{N}_j \qquad [18.12]$$

which has the rank r_j. The goodness-of-fit statistic for solution j was computed as:

$$q_j = \mathbf{d}_J' \mathbf{D}_j^{+} \mathbf{d}_j \qquad [18.13]$$

where $\mathbf{D}_j^{+}$ is the generalised inverse. q_j is expected to follow the χ^2 distribution with r_j degrees of freedom. The global statistic $Q = \sum_j q_j$ should similarly follow the χ^2 distribution with $R = \sum_j r_j$ degrees of freedom.

The procedure for determining the individual weights w_j was roughly as follows. Starting from some *a priori* set of weights, the synthesised solution $\hat{\mathbf{s}}$ was computed according to Equation 18.10, and hence the statistics q_j according to Equations 18.11–18.13. Typically this gave too high a value of Q due to unrealistically small standard errors in some of the individual solutions. The most discrepant solution was identified by comparing the normalised statistics q_j / r_j, the weight of that solution was halved, and a new synthesised solution was computed with revised q_j and Q. This process was iterated until $Q \simeq R$ and all $q_j \simeq r_j$, at which point the synthesised solution $\hat{\mathbf{s}}$ was accepted and assigned the covariance given by the inverse matrix in Equation 18.10.

Method B

This method is based upon the fundamental assumption that the errors obtained by every task are Gaussian. This means that the probability density function is given in its most general form for n variables by:

$$f(x_1, x_2, \ldots, x_n) = (2\pi)^{-n/2} |\mathbf{V}|^{-1/2} \exp \left[-\frac{1}{2} \sum_{i=1}^{n} \sum_{k=1}^{n} \left[\mathbf{V}^{-1} \right]_{ik} (x_i - \overline{x}_i)(x_k - \overline{x}_k) \right] \qquad [18.14]$$

where $\mathbf{V}$ is the variance-covariance matrix of the variables and $\overline{x}_i$ their mean values.

This probability density function can be computed from the data provided by each individual link task (j), namely the estimated variables with their standard errors and the correlation matrix. Now, the joint probability density function of J Gaussian distributions is the product of the probability density functions of these distributions:

$$\varphi = \prod_{j=1}^{J} f_j(x_1, x_2, \ldots, x_n) \qquad [18.15]$$

which is easily computed, and has exactly the same form as Equation 18.14, since the quantities in the exponential add. One can therefore compute back the variance-covariance matrix corresponding to φ and derive the standard errors and the correlations of the merged solution. This approach explicitly assumes Gaussian error distributions and it would not be correct to apply it to other distributions. However, in the particular case to which it is applied, no indication of a non-Gaussian behaviour was given by the individual link solutions which all made the same assumption.

Although formulated in a probabilistic framework, this method is in principle equivalent to a weighted least-squares method and should yield similar results as Method A. However, the practical implementations differ, and Method B was also applied separately to the spin and orientation components, which may add some insight into the properties of the individual solutions. As in Method A, a main problem is to adjust the relative weights of the contributing solutions.

18.7. Synthesis of the Link Solutions: Results

Individual Link Data

The results obtained by various individual solutions were given in three different forms depending on the type of solution:

- if the technique only allowed the determination of the orientation of the Hipparcos frame relative to the extragalactic frame, then the vector $\boldsymbol{\epsilon}(T)$ was given for the mean epoch T of the link observations (MERLIN, VLA, Hamburg/USNO);
- if the technique only allowed the determination of the spin of the Hipparcos frame relative to the extragalactic frame, then only the vector $\boldsymbol{\omega}$ was given (NPM, KSZ, SPM, Bonn, Potsdam);
- if the technique allowed the determination of both the orientation and spin of the Hipparcos frame relative to the extragalactic frame, then the vectors $\boldsymbol{\epsilon}_0$ and $\boldsymbol{\omega}$ were given, with the former referring to the fixed epoch T_0 = J1991.25 (VLBI, HST/FGS, EOP).

In each case the standard errors and the associated covariance matrix were also supplied. These data (except the correlations) are summarised in Tables 18.3–18.4 in the form of the residuals with respect to the finally adopted solution $\widehat{\boldsymbol{\epsilon}}_0$, $\widehat{\boldsymbol{\omega}}$. For the orientation components in Table 18.3 the given data are the residuals at the mean epoch of observation, i.e. $\boldsymbol{\epsilon}(T) - \widehat{\boldsymbol{\epsilon}}(T)$, where T is the datum in the last column.

Results of Method A

The Heidelberg and Yale analyses of the NPM1 do not represent independent determinations. They were therefore averaged prior to the synthesis, and the more pessimistic standard errors from the Heidelberg analysis were adopted for the average. Similarly the blue and visual SPM solutions were averaged, but in this case giving more weight to the blue solutions. Thus, effectively 12 different solutions were considered in this synthesis.

In a first attempt the original standard errors supplied by the different groups were retained; i.e., $w_j = 1$ was adopted for all j. This gave a value of $\simeq 324$ for the χ^2 variable Q, with $R = 44$ degrees of freedom. This shows that the individual solutions are quite incompatible if the given standard errors are taken at face value. Consequently it was necessary to reduce the weights of at least some solutions. It is interesting to note, however, that even this initial weighting gave a solution that was within 1.5 mas in orientation and 0.2 mas/yr in spin from the final one.

The semi-automatic procedure described in the previous section was used for the down-weighting. It is not obvious that this process converges to a unique result. Indeed, slightly different weights were obtained if the starting point was taken at some *a priori* judgement of the relative weights. However, the various synthesised solutions resulting from such experiments rarely differed by more than 0.1 mas and 0.1 mas/yr, and the final result was not very sensitive to additional changes in the weights. Independent of the starting point, it was found that the solutions from the SPM programme and the Earth orientation parameters had to be severely down-weighted, and the Bonn and HST/FGS solutions slightly down-weighted, but otherwise the given standard errors were roughly consistent with the overall solution. The final goodness-of-fit was $Q = 47.9$ with $R = 44$ degrees of freedom; the resulting standard errors of the orientation and spin parameters were multiplied by the unit-weight error, $(Q/R)^{1/2} = 1.043$, to take into account the remaining excess in Q.

The results of Method A are summarised by the following rotation parameters (with standard errors in parentheses) referred to the epoch J1991.25:

$$\left.\begin{aligned} \varepsilon_{0x} &= +0.01\ (0.46)\ \text{mas} \\ \varepsilon_{0y} &= -0.20\ (0.47)\ \text{mas} \\ \varepsilon_{0z} &= +0.12\ (0.49)\ \text{mas} \\ \omega_x &= +0.06\ (0.16)\ \text{mas/yr} \\ \omega_y &= -0.05\ (0.15)\ \text{mas/yr} \\ \omega_z &= +0.00\ (0.14)\ \text{mas/yr} \end{aligned}\right\} \quad \text{A} \qquad [18.16]$$

The correlation matrix for the solution was:

$$\mathbf{R}_{\text{A}} = \begin{pmatrix} 1 & +0.25 & +0.05 & -0.04 & -0.01 & +0.00 \\ +0.25 & 1 & -0.13 & +0.01 & -0.11 & +0.01 \\ +0.05 & -0.13 & 1 & +0.01 & +0.01 & -0.06 \\ -0.04 & +0.01 & +0.01 & 1 & +0.05 & -0.16 \\ -0.01 & -0.11 & +0.01 & +0.05 & 1 & -0.16 \\ +0.00 & +0.01 & -0.06 & -0.16 & -0.16 & 1 \end{pmatrix} \qquad [18.17]$$

The relative contributions of the various link techniques to the synthesised solution can be estimated from the diagonal elements of the re-weighted information matrices $w_j\mathbf{N}_j$. It turns out that for the orientation parameters, the VLBI observations dominate strongly. For the determination of the spin, the contributions are more evenly spread among the several techniques, but with the SPM programme and the VLBI observations together contributing about half of the total weight. It should be noted that in this method the MERLIN, VLA, Hamburg/USNO and HST/FGS links also contribute to the determination of the spin components by virtue of the spread in their mean observational epochs.

Results of Method B

For this method the down-weighting was essentially based upon the considerations given in Section 18.5, moderated by the examination of how the modifications of the weights affected the goodness-of-fit of the synthesised solution and the individual residuals. To begin with, the four solutions obtained from the Yale SPM programme were reduced into a single one by taking a weighted mean. The HST/FGS results for $\boldsymbol{\omega}$ were not used because of their large uncertainties.

In a first approximation, an unweighted solution for $\boldsymbol{\varepsilon}_0$ and another solution for $\boldsymbol{\omega}$ were computed neglecting the correlations between these quantities. This is justified because they are close to zero in the case of the most accurate method (VLBI), but less justified for the Earth orientation parameters method in which the correlations are about 0.89; in this case the uncertainties are also much larger.

In further iterations weights were modified progressively in order to reduce the largest residuals and the overall goodness-of-fit, as measured by the χ^2 statistic. No systematic procedure was used to modify the weights, but rather a successive approximation technique with steps of 0.2 in the weights.

Then, a global solution taking as unknowns all the six parameters of $\boldsymbol{\varepsilon}_0$ and $\boldsymbol{\omega}$ was made, starting with the weights obtained in the preceding solutions. This did not change significantly the results, as can be seen from the following summary of the different solutions.

B1. Solution for $\boldsymbol{\varepsilon}_0$ only: The weighted rms residual was 0.8 mas. The solution vector for the epoch J1991.25 was (standard errors in parentheses):

$$\left.\begin{aligned} \varepsilon_{0x} &= 0.00\ (0.51)\ \text{mas} \\ \varepsilon_{0y} &= -0.04\ (0.51)\ \text{mas} \\ \varepsilon_{0z} &= +0.16\ (0.53)\ \text{mas} \end{aligned}\right\} \quad \text{B1} \qquad [18.18]$$

with correlation matrix:

$$\mathbf{R}_{\text{B1}} = \begin{pmatrix} 1 & +0.28 & -0.01 \\ +0.28 & 1 & -0.14 \\ -0.01 & -0.14 & 1 \end{pmatrix} \qquad [18.19]$$

B2. Solution for $\boldsymbol{\omega}$ only: The weighted rms residual was 0.3 mas/yr. The solution vector was:

$$\left.\begin{aligned} \omega_x &= -0.01\ (0.13)\ \text{mas/yr} \\ \omega_y &= +0.08\ (0.13)\ \text{mas/yr} \\ \omega_z &= -0.05\ (0.18)\ \text{mas/yr} \end{aligned}\right\} \quad \text{B2} \qquad [18.20]$$

with correlation matrix:

$$\mathbf{R}_{\mathrm{B2}} = \begin{pmatrix} 1 & +0.04 & -0.11 \\ +0.04 & 1 & -0.14 \\ -0.11 & -0.14 & 1 \end{pmatrix} \qquad [18.21]$$

B3. Solution for both $\boldsymbol{\varepsilon}_0$ and $\boldsymbol{\omega}$: the weighted rms residual was 1.2 mas for the orientation components and 0.4 mas/yr for the spin components. The solution vectors were:

$$\left.\begin{aligned} \varepsilon_{0x} &= +0.16\ (0.41)\ \mathrm{mas} \\ \varepsilon_{0y} &= +0.18\ (0.43)\ \mathrm{mas} \\ \varepsilon_{0z} &= -0.06\ (0.46)\ \mathrm{mas} \\ \omega_x &= -0.06\ (0.08)\ \mathrm{mas/yr} \\ \omega_y &= +0.05\ (0.09)\ \mathrm{mas/yr} \\ \omega_z &= \ \ 0.00\ (0.14)\ \mathrm{mas/yr} \end{aligned}\right\} \ \mathrm{B3} \qquad [18.22]$$

with correlation matrix:

$$\mathbf{R}_{\mathrm{B3}} = \begin{pmatrix} 1 & +0.03 & +0.00 & +0.31 & +0.08 & -0.36 \\ +0.03 & 1 & -0.13 & +0.10 & +0.13 & -0.25 \\ +0.00 & -0.13 & 1 & -0.01 & -0.02 & +0.00 \\ +0.31 & +0.10 & -0.01 & 1 & -0.11 & -0.07 \\ +0.08 & +0.13 & -0.02 & -0.11 & 1 & -0.12 \\ -0.36 & -0.25 & +0.00 & -0.07 & -0.12 & 1 \end{pmatrix} \qquad [18.23]$$

The correlations obtained in solutions B1 and B2 agree rather well with those obtained from Method A, while the correlations in B3 deviate somewhat. However, the correlations are in all cases small or only moderately large, showing that the combination of link solutions gives a well-conditioned determination of all the parameters at the central epoch of the Hipparcos Catalogue.

Final Results

After a comparison of these results and their discussion, it appeared that a mean value of the two methods should be considered as the final solution for the link. The adopted orientation and rotation vectors for the provisional catalogue H37C, given in Table 16.8, were derived from a combination of the solutions A and B3. In the conventions of the present chapter, where all results are given as residuals with respect to the adopted solution, this corresponds to all parameters equal to zero.

The standard errors of the parameters were estimated to be 0.6 mas in each of the components of $\boldsymbol{\varepsilon}_0$, and 0.25 mas/yr in the components of $\boldsymbol{\omega}$. These numbers were obtained by a conservative rounding of the formal errors resulting from the synthesis, taking into account also the spread of values obtained in the different synthesis solutions and the uncertainty in the relative weights of the different link techniques.

18.8. Verification and Conclusions

A completely independent and accurate verification of the extragalactic link is not possible at present, as practically all available means were already employed in the link. With one important exception, the checks that are at hand can at best demonstrate that the adopted link is not inconsistent with independent data. The exception is the use of stellar kinematics, which is in principle very powerful, but depends on a very simplified statistical description of the Galaxy. This section summarises the independent checks made after the construction of the final Hipparcos Reference Frame.

3C273 (HIP 60936)

The only quasar included in the Hipparcos observing programme was 3C273. Its median magnitude during the mission was $Hp \simeq 12.8$ mag. In addition to its faintness, the position near the ecliptic and equator was quite unfavourable for observation. As a consequence, the standard errors in the five astrometric parameters were in the range 4 to 6 mas or mas/yr. The measured parallax, $\pi = 3.59 \pm 6.07$ mas, is consistent with the assumed cosmological distance (the latter implying a parallax of the order of 10^{-9} arcsec). The position and proper motion measured for this object by Hipparcos were not used in the link, and therefore constitute a completely independent check. The proper motion components measured by Hipparcos, $\mu_{\alpha*} = -11.01 \pm 6.74$ mas/yr and $\mu_\delta = +4.38 \pm 4.28$ mas/yr (with a correlation coefficient of -0.49) are hardly significant: the probability of having errors as large as these is 0.19 in the normal case. It is possible that variable source structure could contribute to the measured proper motion at the level of 0.5 mas/yr.

The offset of the Hipparcos position from the ICRF position of the radio source 3C273B (= ICRF J122906.70+020308.6) is $\Delta\alpha* = +9.61 \pm 7.14$ mas, $\Delta\delta = -2.12 \pm 5.44$ mas, where the standard errors are the quadratically combined standard errors of the positions in the two catalogues. The difference from zero offset is not statistically significant. The rather strong negative correlations between the position and proper motion components ($\rho_{\alpha*}^{\mu_{\alpha*}} = -0.68$, $\rho_\delta^{\mu_\delta} = -0.62$), in combination with the standard errors, show that the effective epoch of observation was close to J1991.85 (see Equation 1.2.10 of Volume 1). At that epoch the offset of the Hipparcos result from the radio position was only $\Delta\alpha* = +3.00 \pm 5.41$ mas, $\Delta\delta = +0.51 \pm 4.63$ mas. This strengthens the conclusion that the proper motion derived from the Hipparcos data is mainly due to noise in the observations, rather than a real motion of the photocentre due to variability.

Magellanic Clouds

Standard models of the motions of the Magellanic Clouds assume that they lead the Magellanic Stream, a narrow band of neutral hydrogen extending some 100° away from the clouds, which then defines the orbit and direction of motion of the clouds. The models predict proper motions of about 1.5 to 2 mas/yr (see Westerlund 1995 for a review). The mean proper motions of the Clouds as derived from the Hipparcos data are consistent in direction and magnitude, to within about 0.4 mas/yr, with e.g. the numerical model by Gardiner *et al.* (1994).

Stellar Kinematics

Galactic kinematics can be used to define an inertial frame based on a statistical model of stellar motions. In the simplest form, the main assumption is that the peculiar motions of the stars are, in a statistical sense, symmetric with respect to the galactic plane. The velocity components *along* the galactic plane are highly systematic and cannot be used to define an inertial frame based on simple kinematical considerations. Consequently only the component of the proper motion in galactic latitude, μ_b, is useful for this purpose.

Let $\mathbf{v}$ and $\mathbf{v}_\odot$ be the peculiar velocities of the star and the Sun, respectively, and $\mathbf{u}$ the unit vector from the Sun towards the star. If the Hipparcos frame is rotating with angular velocity $\boldsymbol{\omega}$, then the observed proper motion vector of the star is given by:

$$\boldsymbol{\mu} = (\mathbf{U} - \mathbf{u}\mathbf{u}')(\mathbf{v} - \mathbf{v}_\odot)\pi/A - \boldsymbol{\omega} \times \mathbf{u} + \boldsymbol{\xi} \qquad [18.24]$$

where $\mathbf{U}$ is the unit tensor, π is the parallax, A the astronomical unit, and $\boldsymbol{\xi}$ represents the error of observation. With $\mathbf{p}_\mathrm{G}$ and $\mathbf{q}_\mathrm{G}$ denoting the unit vectors respectively in the directions of increasing galactic longitude and latitude (Volume 1, Equation 1.5.15), then $\mu_b = \mathbf{q}_\mathrm{G}'\boldsymbol{\mu}$ or:

$$\mu_b = -\mathbf{p}_\mathrm{G}'\boldsymbol{\omega} - \mathbf{q}_\mathrm{G}'\mathbf{v}_\odot\pi/A + v_b\pi/A + \xi_b \qquad [18.25]$$

where $v_b = \mathbf{q}_\mathrm{G}'\mathbf{v}$ is the latitude component of the star's peculiar velocity, and $\xi_b = \mathbf{q}_\mathrm{G}'\boldsymbol{\xi}$ is the observational error in galactic latitude.

Under the assumption that v_b and ξ_b are independent centred random variables with approximately known standard deviations, Equation 18.25 can be used in a least-squares determination of $\boldsymbol{\omega}$ and $\mathbf{v}_\odot$ from the observed values of μ_b and π. Noting that $\mathcal{G}'\mathbf{p}_\mathrm{G} = (-\sin l \;\; \cos l \;\; 0)'$ and $\mathcal{G}'\mathbf{q}_\mathrm{G} = (-\sin b \cos l \;\; -\sin b \sin l \;\; \cos b)'$, where $\mathcal{G} = [\,\mathbf{x}_\mathrm{G} \;\mathbf{y}_\mathrm{G} \;\mathbf{z}_\mathrm{G}\,]$ is the galactic triad, it is seen that only the first two components of $\mathcal{G}'\boldsymbol{\omega}$ may be determined in such a solution, while $\mathbf{z}_\mathrm{G}'\boldsymbol{\omega}$ obviously cannot be estimated from the proper motions in latitude; in contrast, the complete vector of the solar peculiar velocity can be determined.

The Hipparcos proper motions and parallaxes for practically all the 'single' stars were used in a robust least-squares solution based on Equation 18.25, assuming a standard deviation of 25 km s^{-1} for v_b. The results for the first two galactic components of $\boldsymbol{\omega}$ were:

$$\begin{aligned} \omega_1 &\equiv \mathbf{x}_\mathrm{G}'\boldsymbol{\omega} = -0.15 \pm 0.04 \text{ mas/yr} \\ \omega_2 &\equiv \mathbf{y}_\mathrm{G}'\boldsymbol{\omega} = -0.09 \pm 0.05 \text{ mas/yr} \end{aligned} \qquad [18.26]$$

Using different selections of stars depending on distance, galactic latitude or colour gives results within ±0.2 mas/yr of the values above. This result is consistent with the adopted link in $\boldsymbol{\omega}$ and its estimated uncertainty of 0.25 mas/yr in each coordinate.

Graphical Summary

Figures 18.5–18.6 illustrate the verification results from 3C273 and stellar kinematics in the galactic x and y coordinates, together with the results of the various link solutions from Tables 18.3–18.4. Considering the spread of the individual solutions and their formal standard errors (shown by error circles or bands), the results from 3C273 and stellar kinematics are fully consistent with the link solutions and with the adopted mean result (represented by the origin of each diagram) to within its stated uncertainty.

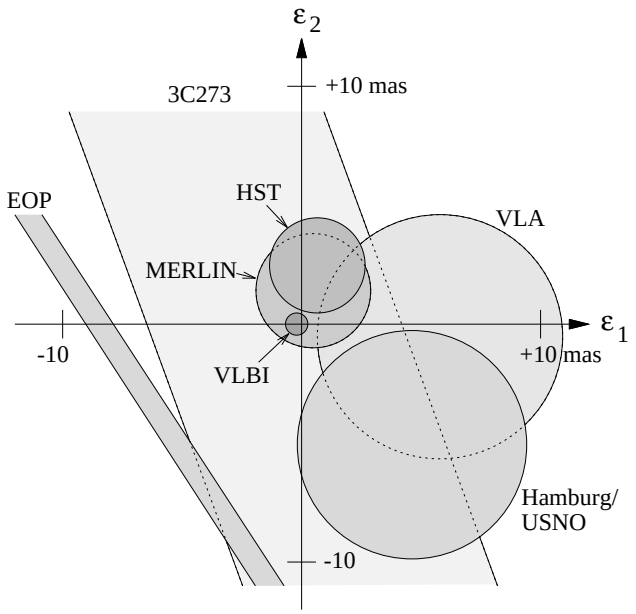

Figure 18.5. *Summary of the results for the orientation vector* $\boldsymbol{\varepsilon}$*, expressed in the galactic x and y coordinates* ($\varepsilon_1 = \mathbf{x}'_G\boldsymbol{\varepsilon}$ *and* $\varepsilon_2 = \mathbf{y}'_G\boldsymbol{\varepsilon}$)*. The individual results from Table 18.3 are shown as error circles with a radius of one standard deviation. In the case of the Earth orientation parameters, only two of the equatorial components of* $\boldsymbol{\varepsilon}$ *were determined, defining a band in the* $(\varepsilon_1, \varepsilon_2)$ *plane corresponding to the* $\pm 1\sigma$ *uncertainty. The verification result from the position of 3C273 at its mean epoch of observation is also shown as a band corresponding to its* $\pm 1\sigma$ *uncertainty.*

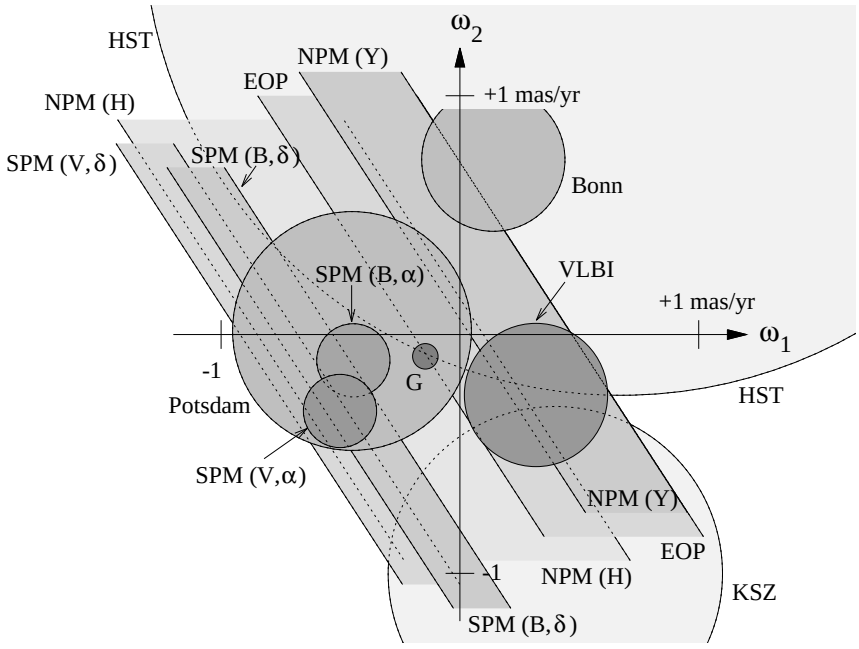

Figure 18.6. *Summary of the results for the spin vector* $\boldsymbol{\omega}$*, expressed in the galactic x and y coordinates* ($\omega_1 = \mathbf{x}'_G\boldsymbol{\omega}$ *and* $\omega_2 = \mathbf{y}'_G\boldsymbol{\omega}$)*. The individual results from Table 18.4 are shown as error circles with a radius of one standard deviation. In cases where only two equatorial components of* $\boldsymbol{\omega}$ *were determined, the corresponding uncertainty bands (of width* $\pm 1\sigma$*) are shown. The verification result from galactic kinematics, Equation 18.26, is shown by the error circle labelled* 'G'.

Conclusions

The procedure for determining the Hipparcos Reference Frame strictly followed the IAU intentions for the new conventional celestial reference system, namely that it should be non-rotating with respect to distant matter and that the fundamental directions are set by the precise coordinates of extragalactic radio sources. As a matter of principle, the procedure was not allowed to be influenced by considering the relationship to the dynamical reference frame of the solar system or to the kinematical frame defined by motions in our Galaxy.

Such considerations could nevertheless be applied *a posteriori* as a check of the Hipparcos Reference Frame. For instance, observations of solar system objects in the Hipparcos frame, together with a dynamical theory of the planetary motions, will determine the direction of the total angular momentum of the solar system, which is expected to remain fixed in the extragalactic frame to very high accuracy. This check must however await a detailed (re-)analysis of the solar system observations, both from Hipparcos and from the ground.

The various checks described in this section are all consistent with the stated accuracy of the extragalactic link, namely 0.6 mas in the orientation and 0.25 mas/yr in the spin, although no significant test of the orientation was obtained by these methods. The strongest test of the spin is provided by the galactic kinematics, supporting the conclusion that the Hipparcos frame is inertial to within a few tenths of a milliarcsec per year.

18.9. Organisation of the Work

The importance of linking the Hipparcos Catalogue to the extragalactic system was stressed already in the planning of the observing programme. Extensive preparations were made by the INCA Consortium to initiate and collect relevant ground-based observations of radio stars and stars in the fields of compact extragalactic radio sources, and to ensure that suitable link stars were included on the observing list (Argue 1989, 1991; Jahreiß *et al.* 1992). A special working group for the determination of the extragalactic link was appointed by the Hipparcos Science Team in 1993. It contained representatives of all the groups participating in the link observations and was coordinated by J. Kovalevsky and L. Lindegren, who were also responsible for the synthesis of the different link determinations.

The members of the various groups contributing to the determination of the link are listed hereafter.

VLBI: J.F. Lestrade led this group in close collaboration with R.A. Preston, D.L. Jones (JPL) and R.B. Phillips (Haystack) for the northern stars, and J. Reynolds, D. Jauncey (CSIRO) and J.C. Guirado (JPL) for the southern hemisphere.

MERLIN: This group comprised S.T. Garrington and R.J. Davis (NRAL, Jodrell Bank), L.V. Morrison and R.W. Argyle (RGO), and A.N. Argue (IoA, Cambridge).

VLA: This task was organised by K.J. Johnston (USNO); the computation of the link was done by D.R. Florkowski (USNO).

Hamburg/USNO: This link was realised by C. de Vegt (Hamburg) and N. Zacharias (USNO).

HST/FGS: Based on observations with the NASA/ESA Hubble Space Telescope, this work was carried out by many people, but the data collection and analysis was the result of continued efforts of P.D. Hemenway, E.P. Bozyan, R.L. Duncombe, A. Lalich, B. MacArthur, E. Nelan and the Hubble Space Telescope Team.

Lick (NPM): The analysis of the NPM1 data for the Hipparcos link was made at Yale Observatory by I. Platais, T.M. Girard, and V. Kozhurina-Platais, and at the Astronomisches Rechen-Institut, Heidelberg, by S. Röser.

Catalogue of Faint Stars (KSZ): This link was realised at Kiev Observatory by N.V. Kharchenko, V.S. Kislyuk, S.P. Rybka and A.I. Yatsenko.

Yale/San Juan (SPM): This work was shared by I. Platais, T.M. Girard, V. Kozhurina-Platais; H.T. MacGillivray and D.J. Yentis furnished positions and magnitudes from the COSMOS/UKST data base of the southern sky and W.F. van Altena provided many useful suggestions.

Bonn: This work was shared by H.-J. Tucholke, P. Brosche, M. Geffert, M. Hiesgen (Münster), A. Klemola (Lick), M. Odenkirchen and J. Schmoll.

Potsdam: This link was realised by E. Schilbach, S. Hirte and R.-D. Scholz.

Earth Orientation Parameters: This task was performed by J. Vondrák, I. Pešek and C. Ron.

J. Kovalevsky, L. Lindegren, M.A.C. Perryman